Optimal diagnostic approach for using CT-derived quantitative flow ratio in patients with stenosis on coronary computed tomography angiography

Dahl, Jonathan N.; Rasmussen, Laust D.; Ding, Daixin; Tu, Shengxian; Westra, Jelmer; Wijns, William; Christiansen, Evald Høj; Eftekhari, Ashkan; Li, Guanyu; Winther, Simon; Bøttcher, Morten

Published in:
Journal of Cardiovascular Computed Tomography

DOI (link to publication from Publisher):
10.1016/j.jcct.2024.01.004

Publication date:
2024

Document Version
Publisher's PDF, also known as Version of record

Journal of Cardiovascular Computed Tomography 18 (2024) 162–169

Contents lists available at ScienceDirect

Journal of Cardiovascular Computed Tomography

journal homepage: www.JournalofCardiovascularCT.com

Research paper

Optimal diagnostic approach for using CT-derived quantitative flow ratio in patients with stenosis on coronary computed tomography angiography

Jonathan N. Dahl [a,b,*], Laust D. Rasmussen [a,b,c], Daixin Ding [d,e], Shengxian Tu [e,f], Jelmer Westra [b,g], William Wijns [d], Evald Høj Christiansen [b,g], Ashkan Eftekhari [c], Guanyu Li [e], Simon Winther [a,b], Morten Bøttcher [a,b]

[a] Department of Cardiology, Gødstrup Hospital, Herning, Denmark
[b] Department of Clinical Medicine, Aarhus University, Aarhus, Denmark
[c] Department of Cardiology, Aalborg University Hospital, Aalborg, Denmark
[d] The Lambe Institute for Translational Research and Curam, University of Galway, Ireland
[e] Biomedical Instrument Institute, School of Biomedical Engineering, Shanghai Jiao Tong University, China
[f] Med-X Research Institute, Shanghai Jiao Tong University, Shanghai, China
[g] Department of Cardiology, Aarhus University Hospital, Denmark

ARTICLE INFO

Keywords:
Computed tomography derived quantitative flow reserve
Coronary artery disease
Coronary computed tomography angiography
Fractional flow reserve
Non-invasive cardiac imaging
Quantitative coronary analysis

ABSTRACT

Background: Coronary computed tomography angiography (CCTA)-derived quantitative flow ratio (CT-QFR) is an on-site non-invasive technique estimating invasive fractional flow reserve (FFR). This study assesses the diagnostic performance of using most distal CT-QFR versus lesion-specific CT-QFR approach for identifying hemodynamically obstructive coronary artery disease (CAD).

Methods: Prospectively enrolled de novo chest pain patients (n = 445) with ≥50 % visual diameter stenosis on CCTA were referred for invasive evaluation. On-site CT-QFR was analyzed post-hoc blinded to angiographic data and obtained as both most distal (MD-QFR) and lesion-specific CT-QFR (LS-QFR). Abnormal CT-QFR was defined as ≤0.80. Hemodynamically obstructive CAD was defined as invasive FFR ≤0.80 or ≥70 % diameter stenosis by 3D-quantitative coronary angiography.

Results: In total 404/445 patients had paired CT-QFR and invasive analyses of whom 149/404 (37 %) had hemodynamically obstructive CAD. MD-QFR and LS-QFR classified 188 (47 %) and 165 (41 %) patients as abnormal, respectively. Areas under the receiver-operating characteristic curve for MD-QFR was 0.83 vs. 0.85 for LS-QFR, p = 0.01. Sensitivities for MD-QFR and LS-QFR were 80 % (95%CI: 73–86) vs. 77 % (95%CI: 69–83), p = 0.03, respectively, and specificities were 73 % (95%CI: 67–78) vs. 80 % (95%CI: 75–85), p < 0.01, respectively. Positive predictive values for MD-QFR and LS-QFR were 63 % vs. 69 %, p < 0.01, respectively, and negative predictive values for MD-QFR and LS-QFR were 86 % vs. 85 %, p = 0.39, respectively).

Conclusion: Using a lesion-specific CT-QFR approach has superior discrimination of hemodynamically obstructive CAD compared to a most distal CT-QFR approach. CT-QFR identified most cases of hemodynamically obstructive CAD while a normal CT-QFR excluded hemodynamically obstructive CAD in the majority of patients.

Abbreviations: 3D-QCA, 3-Dimensional-quantiative invasive coronary angiography analysis; CACS, Coronary artery calcium score; CAD, Coronary artery disease; CCTA, Coronary computed tomography angiography; CT-QFR, Computed tomography derived quantitative flow ratio; DS, Diameter stenosis; FFR, Fractional flow reserve; ICA, Invasive coronary angiography; MLD, Minimal Lumen diameter; PCI, Percutaneous coronary intervention; RLD, Reference Lumen diameter.

* Corresponding author. Hospitalsparken 15, 7400 Herning, Denmark.
E-mail addresses: jonadh@rm.dk (J.N. Dahl), laust.dupont@midt.rm.dk (L.D. Rasmussen), d.ding2@nuigalway.ie (D. Ding), sxtu@sjtu.edu.cn (S. Tu), jelwes@rm.dk (J. Westra), william.wyns@nuigalway.ie (W. Wijns), evald.christiansen@rm.dk (E.H. Christiansen), asef@rn.dk (A. Eftekhari), guanyu.li@sjtu.edu.cn (G. Li), sw@dadlnet.dk (S. Winther), morboett@rm.dk (M. Bøttcher).

https://doi.org/10.1016/j.jcct.2024.01.004
Received 12 September 2023; Received in revised form 27 December 2023; Accepted 6 January 2024
Available online 18 January 2024

1. Introduction

1.1. Background

In de novo chest pain patients with suspected obstructive coronary artery disease (CAD), initial non-invasive testing by coronary computed tomography angiography (CCTA) is recommended to rule out obstructive CAD, in particular in lower pre-test likelihood patients.[1–3] However, the correlation between stenosis severity on CCTA and flow limitation measured invasively is only moderate,[4] and two in five patients consequently undergo revascularization when referred for an invasive investigation following a CCTA with suspected obstructive stenosis.[5] Therefore, second-line functional imaging is recommended before invasive referral.[2,3,6]

Computational physiology models derived from different coronary imaging modalities have been developed to estimate the functional significance of a suspected coronary stenosis.[7–10] Quantitative flow ratio (QFR), a method for fast estimation of invasive fractional flow reserve (FFR) from invasive coronary angiography (ICA), was recently validated with good agreement to invasive FFR.[11–13] Recently, the QFR algorithm has been modified and applied to CCTA images for non-invasive estimation of FFR (CT-QFR) with equally good agreement and diagnostic performance compared to invasive FFR.[9,14,15]

Thus, in patients with suspected stenosis on coronary CTA, second-line functional imaging using CT-QFR holds the potential to increase revascularization rates at ICA in patients selected by CCTA. However, the validity of existing evidence of CT-QFR performance is limited to central core-lab evaluations of mainly retrospective registries, and non-invasive CT-QFR values have previously only been reported for invasively interrogated vessels. Hence, the non-invasive applicability of CT-QFR to guide referral for downstream ICA is unknown.[9,14,15] Additionally, though CT-QFR can be measured throughout the span of a coronary artery, only distal vessel values have been utilized without stenosis or pressure-wire location adjudication which could potentially affect values of CT-QFR and hence diagnostic performance.[16]

1.2. Objective

In patients with suspected stenosis on CCTA, we aimed to 1) assess the diagnostic performance of second line on-site CT-QFR against hemodynamically obstructive CAD by invasive FFR, and 2) compare the diagnostic performance of using most distal (MD-QFR) versus lesion-specific (LS-QFR) CT-QFR measurements.

2. Methods

2.1. Study population and study overview

This is a post-hoc sub-study of the Danish study of Non-Invasive testing in Coronary Artery Disease 2 (Dan-NICAD 2. ClinicalTrials ID: NCT03481712); a prospective, multicenter, cross-sectional study including 1732 symptomatic de novo chest pain patients without previously known CAD referred for CCTA by clinical indication. The study protocol and main findings were previously reported.[17,18] In short, patients with suspected stenosis on CCTA (≥50 % diameter stenosis (DS)) were referred for second-line non-invasive stress imaging and subsequent invasive FFR (Fig. 1).

The present paper investigates the diagnostic performance of CT-QFR against hemodynamically obstructive CAD by invasive FFR in patients with ≥50 % diameter stenosis (DS) on CCTA. First, MD-QFR and LS-QFR measurements were performed on-site and blinded to patient demographics, non-invasive stress imaging and ICA results (Fig. 1). Secondly, CT-QFR measurements were adjudicated to images of the location of the pressure wire sensor during ICA. Third, diagnostic performance of

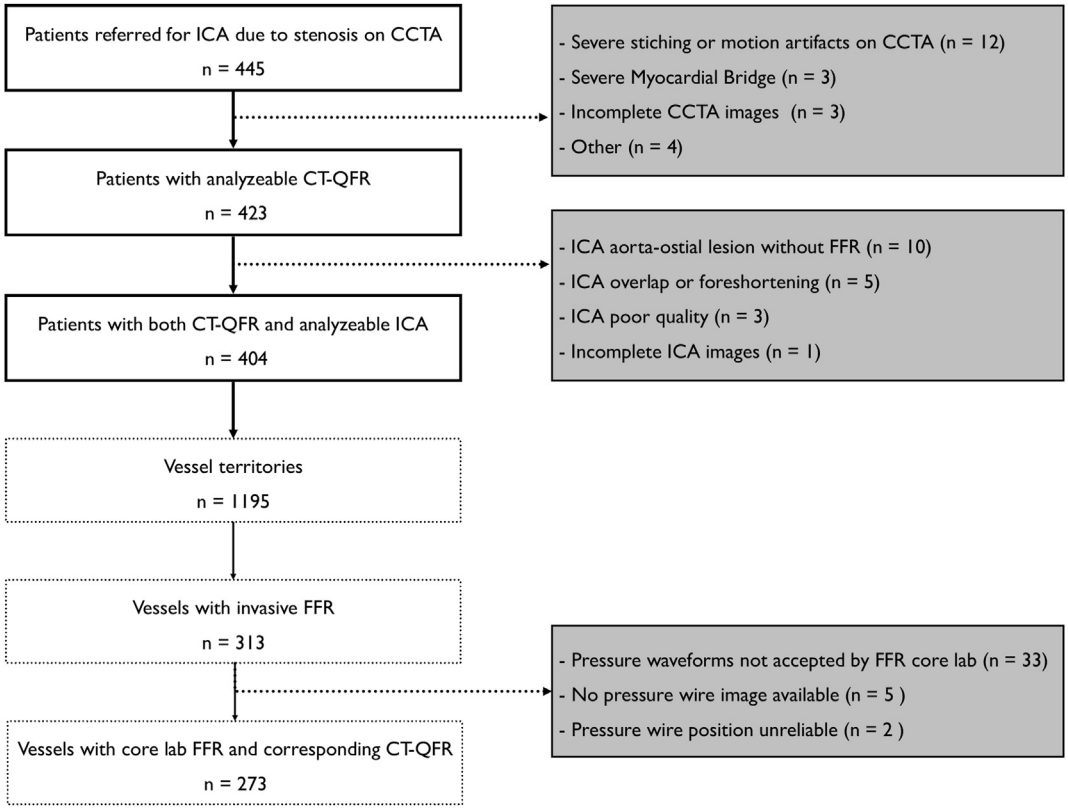

Fig. 1. Consort diagram. In total, 1722 patients completed CCTA, with 445 (26 %) having >50 % diameter stenosis, all 445 underwent ICA. The final study cohort (n = 404) represents patients who completed CCTA, and had paired CT-QFR and ICA analyses.

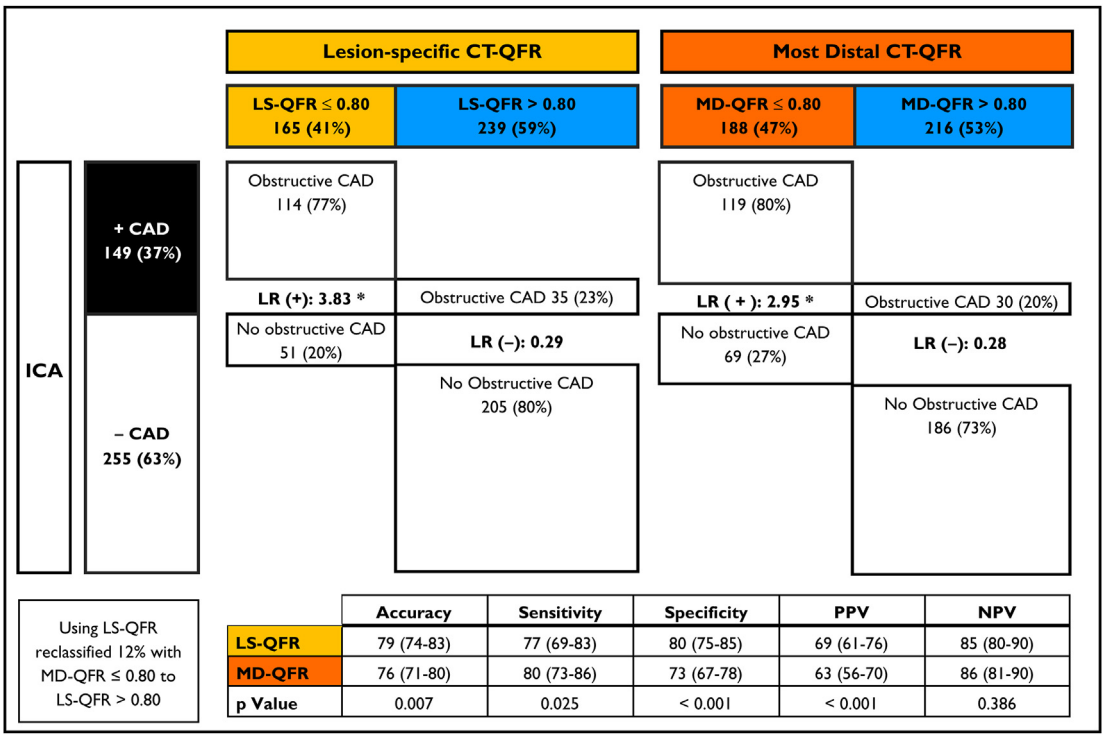

Fig. 2. Contigency table for the two different CT-QFR approaches. Graphical representation of 2 × 2 contingency table over lesion-specific and most distal CT-QFR according to presence or absence of hemodynamically obstructive CAD on ICA. Box sizes corresponds to prevalence. * denote P < 0.001 between positive likelihood ratios (LR (+)); P = 0.393 between negative likelihood ratios (LR (−)).

MD-QFR and LS-QFR against hemodynamically obstructive CAD on ICA were investigated on a per-patient and a per-vessel level. Finally, correlations and agreements between measurements of CT-QFR with invasive FFR were investigated.

The study followed the principles of the Declaration of Helsinki and ISO 14155:2011.

2.2. Coronary CTA exclusion criteria for CT-QFR analysis

Exclusion criteria for this study was: 1) non-diagnostic Image quality defined as reduced image quality which precluded appropriate evaluation of the coronary arteries (Grade 1 Likert image quality[19]); 2) incomplete CCTA examinations, precluding full-vessel evaluation of all coronary arteries ≥1.5 mm[9]; and 3) vessels with severe myocardial bridging defined as complete vessel encasement in the myocardium, depth ≥2 mm, and length >10 mm in the interrogated vessel on CCTA.

2.3. Computed tomography acquisition and interpretation

The acquisition and interpretation of CCTA were previously described.[17] First, a coronary artery calcium score (CACS) was calculated for all patients using non-enhanced images. Secondly, a contrast-enhanced examination enabled evaluation of stenosis severity using an 18-segment model of the coronary tree.[20]

Suspected obstructive CAD on CCTA was defined as visual DS ≥ 50 % by a reading expert physician, while a severe stenosis on CCTA was defined as visual DS ≥ 70 %.[20]

2.4. Computation of CT-QFR

The methodological principles of CT-QFR computation have previously been described.[9,14,15,21] In short, CCTA images were analyzed by an external analyst blinded to any procedural results. Analyses were performed on-site on local hardware by a trained reader certified in CT-QFR computation by the technology provider. The software version of the CT-QFR was CtaPlus V2 (Pulse Medical, China) which enabled semi-automatic lumen extraction with manual corrections allowed if needed. A more detailed description of the applied CT-QFR approach is outlined in the Supplemental Data.

Following CT-QFR computation, MD-QFR values were extracted most distally in all coronary arteries ≥1.5 mm regardless of the presence or location of any stenosis. LS-QFR values were extracted just at the distal border of a stenotic lesion using the automatic detection limit of 20 % luminal DS with manual adjudication (Graphical Abstract). After all CT-QFR analyses were completed, ICAs were reviewed, and recordings of the invasive pressure wire sensor location was used to extract pressure wire-adjudicated CT-QFR measurements at the corresponding location, using the 3D coronary tree reconstruction from the CT-QFR analysis.

The primary analyses included per-patient diagnostic evaluations according to MD-QFR and LS-QFR against obstructive CAD on ICA as reference. Secondary analyses included per-patient diagnostic performance of both CT-QFR approaches and a visual 70 % DS threshold on CCTA for detecting obstructive CAD at ICA as reference; an analysis of per-patient diagnostic performance of CT-QFR with revascularization as reference was also performed. Per-vessel CT-QFR diagnostic performance was investigated with vessels categorized according to the three coronary vessel distributaries: left anterior descending artery (LAD) (including the left main (LM) artery), left circumflex artery (LCX) and the right coronary artery (RCA). Additionally, in the vessels with pressure wire interrogation, the correlation and agreement of invasive FFR with both MD-QFR and LS-QFR were investigated.

For both the per-patient- and per-vessel analyses, an abnormal MD-QFR and LS-QFR were defined as a value of ≤0.80 or a visually assessed total occlusion (assigned ≤0.80 for both MD- and LS-QFR).[22] Patient level MD-QFR and LS-QFR were the lowest values measured in any artery; thus, if at least one vessel had MD-QFR or LS-QFR value of

≤0.80, respectively, patients were classified as having obstructive CAD according to the approach. In vessels without detected stenosis by CT-QFR, LS-QFR were regarded as normal (LS-QFR >0.80) regardless of MD-QFR value.

2.5. Invasive coronary angiography and fractional flow reserve

According to the study protocol, invasive FFR was performed if technically possible in lesions with visual 30–90 % DS in vessels >2 mm in diameter during hyperemia using standard adenosine stress protocol. All pressure waveforms were analyzed by a core lab (Interventional Imaging Core Laboratories, Aarhus University, Denmark). If invasive FFR was indicated but not, performed or the pressure waveforms were not accepted, diameter stenosis (DS) severity was assessed using 3D-quantitative coronary angiography (3D-QCA); Medis Suite QAngio XA-3D/QFR solution (Medis Medical Imaging bv., Leiden, The Netherlands). The 3D-QCA analyses additionally provided information on minimal lumen diameter (MLD) and reference lumen diameter (RLD).[18]

For the primary analysis, hemodynamically obstructive CAD was defined as either invasive FFR ≤0.80 or ≥0.70 % diameter stenosis by 3D-QCA (including total occlusion), if invasive FFR was not available.

2.6. Statistical analysis

Continuous variables are expressed as mean with standard deviations (SD) if normally distributed, otherwise as median with total or interquartile range (IQR). Dichotomous or categorical variables are reported as n (%).

The diagnostic performance of MD-QFR and LS-QFR were evaluated by diagnostic accuracy, sensitivity, specificity and compared using McNemar's test. Positive (PPV), negative predictive (NPV) values were calculated and compared by weighted generalized score statistics,[23] positive and negative likelihood ratios were compared using regression models. Area under the receiver operating characteristic curve (AUC) were compared using the Delong method. Furthermore, diagnostic comparisons of MD-QFR and LS-QFR with ≥70 % DS on CCTA with obstructive CAD at ICA as reference were made. Tests were made on both a per-patient and per-vessel level.

The correlation and agreement of CT-QFR with invasive FFR were assessed with Spearman's correlation coefficients, visualized with scatter and Bland-Altman plots.The impact of CACS >400 in vessels with pressure wire interrogation on both correlation and agreement of CT-QFR compared with invasive FFR were investigated.

Finally, in vessels with both invasive FFR, CT-QFR and 3D-QCA, multivariate mixed effect linear regression models were applied to predict differences between invasive FFR and LS-QFR, accounting for different vessels within the same patient. Models based on differences in diameter stenosis, minimal lumen diameter and reference lumen diameter measures on ICA and CT were constructed, with adjustment for heart rate, BMI, vessel territory and vessel CACS.

For all statistical analyses, 95 % confidence intervals (CI) were reported when appropriate and a two-tailed p value < 0.05 was considered statistically significant, in case of multiple comparisons, Bonferroni correction was applied. Statistical analyses were performed using Stata 16 (StataCorp, College Station, Texas) and R (R Foundation for Statistical Computing, Vienna, Austria).

3. Results

3.1. Study population

In total, 1722/1732 (99 %) patients underwent CCTA of whom 445/1722 (26 %) had at least 1 vessel with a ≥50 % diameter stenosis by the clinical site-read. Of these, 423/445 (95.1 %) patients obtained an image quality that allowed for successful CT-QFR analysis of all three major coronary arteries and side branches (Fig. 1). Median CT-QFR analysis time including lumen reconstruction was 9 min with an IQR of 7–12 min. All patients underwent ICA, with 404/423 having complete ICA analyses (Fig. 1). Baseline characteristics and CCTA findings for the final cohort (n = 404) are shown in Table 1.

On a per-patient level, hemodynamically obstructive CAD was identified in 149/404 (36.9 %) patients of whom 90/149 (60.4 %) had invasive FFR ≤0.80 while 59/149 (39.6 %) patients had ≥70 % DS by 3D-QCA alone (Table 2). Overall, 43 patients had multi-vessel disease. On a per-vessel level, hemodynamically obstructive CAD was identified in 193/1195 (16.2 %) vessels (Supplementary Table 1).

3.2. Diagnostic performance of most distal and lesion-specific CT-QFR

Median patient MD-QFR was 0.82 [0.75–0.86], and median patient LS-QFR was 0.83 [0.78–0.90] (Table 2). On a per-patient level, 188/404 (46.5 %) had ≥1 vessel with MD-QFR ≤0.80, and 165/404 (40.8 %) patients had ≥1 vessel with LS-QFR ≤0.80. Thus, 23/188 (12 %) of patients were reclassified as having no hemodynamically obstructive CAD by using LS-QFR rather than MD-QFR (Fig. 2, Graphical Abstract).

Per-patient area under the receiver operating curves were 0.83 (0.79–0.87) for MD-QFR versus vs. 0.85 (0.81–0.89) for LS-QFR, p = 0.005, with overall superior diagnostic accuracy for LS-QFR (79 % vs. 76 % for MD-QFR, p = 0.007). However, MD-QFR showed superior sensitivity compared to LS-QFR (80 % vs. 77 %, p = 0.025) while specificity was impaired (73 % vs. 80 % for LS-QFR, p < 0.001) (Fig. 2, Graphical Abstract). The NPV of MD-QFR was 86 % vs. 85 % for LS-QFR, p = 0.386; whereas, MD-QFR had a lower PPV of 63 % vs. 69 % for LS-QFR, p < 0.001 (Fig. 2, Graphical Abstract). Using a LS-QFR approach would decrease the number of false positives to 20 % from 27 % by MD-QFR (Fig. 2). Of the 43 patients with multi-vessel disease, MD-QFR identified 42 (98 %) as abnormal, while LS-QFR correctly identified 41 (95 %), p = 0.317 (Table 2). Similar results were found by the sensitivity reference of revascularization (n = 155) (Figure S1).

A ≥70 % DS on CCTA was present in 240 (59 %) patients. For identifying obstructive CAD at ICA Sensitivity and NPV were similar between both CT-QFR approaches and ≥70 % DS on CCTA (Table 3). However, AUC (0.66), diagnostic accuracy (63 %) specificity (53 %) and PPV (50 %) were all significantly lower for 70 % DS on CCTA (p < 0.001 for all)

Table 1
Baseline Patient and Imaging Characteristics for final cohort (n = 404).

Characteristic	
Gender, male	285 (70.5 %)
Age, years, mean ± SD	63.4 ± 7.6
Cardiovascular risk factors	
ESC-PTP	0.22 [0.11–0.32]
Family history of early CAD	163 (40.7 %)
Current smoking	131 (32.4 %)
Diabetes mellitus	39 (9.7 %)
Lipid-lowering treatment	61 (15.2 %)
Antihypertension treatment	209 (51.7 %)
Body Mass Index, mean ± SD	27.3 ± 3.8
Symptoms	
Typical chest pain	114 (28.2 %)
Atypical chest pain	143 (35.4 %)
Non-anginal chest pain	91 (22.5 %)
Dyspnea or arrhythmia	56 (13.9 %)
Coronary computed tomography angiography	
Heart rate, beats/min	59 ± 8
Coronary artery calcium score, median [IQR]	293 [97–807]
= 0	29 (7.2 %)
1-399	212 (52.5 %)
≥400	163 (40.4 %)
Maximum stenosis on CCTA ≥ 70 % DS	240 (59.4 %)
Coronary artery disease severity (number of vessels with ≥50 % DS on CCTA)	
- 1-vessel disease	226 (55.9 %)
- 2-vessel disease	99 (24.5 %)
- 3-vessel disease or left main disease	79 (19.6 %)

CCTA: Coronary computed tomography angiography; DS Diameter stenosis; ESC-PTP: European Society of Cardiology Pre-test probability score.

Table 2
ICA and CT-QFR imaging result patient level (n = 404).

ICA	
At least one ≥30 % visual DS	307 (76.0 %)
FFR performed	219 (54.2 %)
Median FFR	0.83 [0.75–0.88]
Obstructive CAD, either:	149 (36.9 %)
- FFR ≤ 0.80	90 (21.3 %)
- 3D-QCA ≥ 70 %	79 (19.6 %)
Non-obstructive CAD	255 (63.1 %)
CAD Severity and location (n = 149)	
- 1-vessel disease	106 (71.1 %)
- 2-vessel disease	32 (21.5 %)
- 3-vessel or LM disease	11 (7.4 %)
- LAD disease	104 (71.7 %)
- LCX disease	33 (23.4 %)
- RCA disease	50 (34.7 %)
CT-QFR	
Median most distal CT-QFR*	0.82 [0.75–0.86]
Most distal CT-QFR > 0.80	216 (53.5 %)
Most distal CT-QFR ≤ 0.80	188 (46.5 %)
Median lesion-specific CT-QFR*	0.83 [0.78–0.90]
Lesion-specific CT-QFR > 0.80	239 (59.2 %)
Lesion-specific CT-QFR ≤ 0.80	165 (40.8 %)

Number (Frequency), or mean ± SD, or median (Interquartile Range). *Exempting occluded vessels at CT-QFR. CT-QFR computed tomography derived quantitative flow ratio, FFR fractional flow reserve, ICA invasive coronary angiography, LAD left anterior descending, LCX left circumflex, LM left main, RCA right coronary artery.

(Table 3). Thus, MD-QFR and LS-QFR reclassified 22 % and 31 % of patients with ≥70 % on CCTA as normal, respectively.

On a per-vessel level, AUCs were similar between MD-QFR and LS-QFR (0.88 vs. 0.88, p = 0.495). In accordance with patient-level analysis, accuracy and specificity were higher for LS-QFR while sensitivity was impaired (Table S1). The per-vessel diagnostic performance of CT-QFR versus ≥70 % DS on CCTA for detecting obstructive CAD at ICA was similar to the patient-level analysis (Table S1).

Table 3
Diagnostic Performance of MD-QFR and LS-QFR and 70 % Diameter Stenosis on CCTA for detecting hemodynamically obstructive CAD at ICA, Patient-level (n = 404).

2 × 2 Contigency Table	CCTA 70 % DS	
	≥70 % DS	<70 % DS
Hemodynamically obstructive CAD at ICA	119	30
No hemodynamically obstructive CAD at ICA	121	134

Patient Level Analysis (n = 404)	MD-QFR	LS-QFR	CCTA 70 % DS
Accuracy	75.5 (71.0–79.6)	78.7 (74.4–82.6)	62.7 (57.8–67.4)*
Sensitivity	79.9 (72.5–86.0)	76.5 (68.9–83.1)	79.9 (72.5–86.0)
Specificity	72.9 (67.0–78.3)	80.0 (74.6–84.7)	52.5 (46.2–58.8)*
PPV	63.3 (56.0–70.2)	69.1 (61.4–76.0)	49.6 (43.1–56.1)*
NPV	86.1 (80.8–90.4)	85.4 (80.2–89.6)	81.7 (74.9–87.3)
LR (+)	2.95 (2.38–3.67)	3.83 (2.95–4.97)	1.68 (1.45–1.96)*
LR (−)	0.28 (0.20–0.38)	0.29 (0.22–0.39)	0.38 (0.27–0.54)
AUC	0.83 (0.79–0.87)	0.85 (0.81–0.89)	0.66 (0.62–0.71)*

Patient-level performance of most distal and lesion-specific CT-QFR and 70 % DS on CCTA. * Indicates p-values <0.001 for MD-QFR and LS-QFR against 70 % DS on CCTA; sensitivity, NPV and negative likelihood ratios comparisons all had p-values > 0.10. DS denotes diameter stenosis. For 2 × 2 contingency tables for MD-QFR and-LS-QFR please see Fig. 2.

If vessels with total occlusions (n = 30) at ICA were excluded from the analysis, the patient level sensitivity was decreased to 70 % for MD-QFR and to 67 % for LS-QFR (p = 0.166), with minor reductions in the other diagnostic metrics (Table S2).

3.3. Pressure wire CT-QFR agreement and correlation to invasive FFR

In total, 273 vessels from 220 patients had paired measurements of CT-QFR and invasive FFR in which median invasive FFR was 0.83 [0.77–0.90] and median CT-QFR at the location of the pressure wire was 0.86 [0.80–0.90] (Table 4). Both CT-QFR at the pressure wire location and LS-QFR were overestimated compared to invasive FFR while MD-QFR showed good agreement with invasive FFR (Fig. 3). Values of CT-QFR at the location of the pressure wire correlated moderately with invasive FFR, rho 0.60, p < 0.001 (Fig. 3). CACS severity did not impact the correlation and agreement of invasive FFR and CT-QFR at the location of the pressure wire (Figure S2).

3.4. Multivariate regression analysis of difference between invasive FFR and LS-QFR

In total, 246 vessels with invasive FFR, LS-QFR and 3D-QCA were available for linear regression modeling using anatomical ICA and CT measures to predict differences between invasive FFR and LS-QFR. Overall, differences in diameter stenosis (β: −0.03/10 % difference in DS assessment, p < 0.001) and minimum lumen diameter (β: 0.05/1 mm difference in MLD assessment, p < 0.001) predicted invasive FFR and LS-QFR discrepancy (Table S3 and Figure S3). Conversely, differences in reference lumen diameter assessment could not explain the invasive FFR and CT-QFR discrepancy (Figure S4).

4. Discussion

This study evaluated the diagnostic performance of CT-QFR as a non-invasive alternative to invasive investigations in patients with suspected obstructive CAD. We found that both MD-QFR and LS-QFR had similar diagnostic accuracy with LS-QFR yielding higher specificity at the cost of lower sensitivity. Furthermore, both CT-QFR approaches had either similar or superior diagnostic performance compared to ≥70 % DS on CCTA for detection of obstructive CAD at ICA. In vessels where both invasive FFR and CT-QFR were measured, CT-QFR measurements overestimated invasive FFR values which could partly be explained by discrepancy in the assessment of anatomical stenosis severity by CT-QFR software and ICA.

Table 4
Vessels with invasive FFR and CT-QFR (n = 273), invasive findings.

	ICA	CT-QFR		
		Pressure wire QFR	LS-QFR	MD-QFR
Median FFR or CT-QFR	0.83 [0.77–0.90]	0.85 [0.80–0.90]	0.86 [0.80–0.91]	0.84 [0.79–0.88]
N (%) ≤ 0.80	101 (37.0 %)	74 (27.1 %)	72 (26.4 %)	91 (33.3 %)
Diameter stenosis, %*	45 [39–51]	37 [30–44]		
Minimal lumen diameter, mm*	1.6 [1.3–1.9]	1.8 [1.5–2.1]		
Reference lumen diameter, mm*	2.9 [2.6–3.3]	2.9 [2.5–3.3]		

Invasive FFR and 3D-QCA findings in vessels with invasive FFR, and the same for CT-QFR in corresponding vessels. Vessels included 160 LAD/LM, 12 diagonal branches, 49 LCX, 52 RCA. * denote available for 246 paired vessels. Abbreviations as in Table 2.

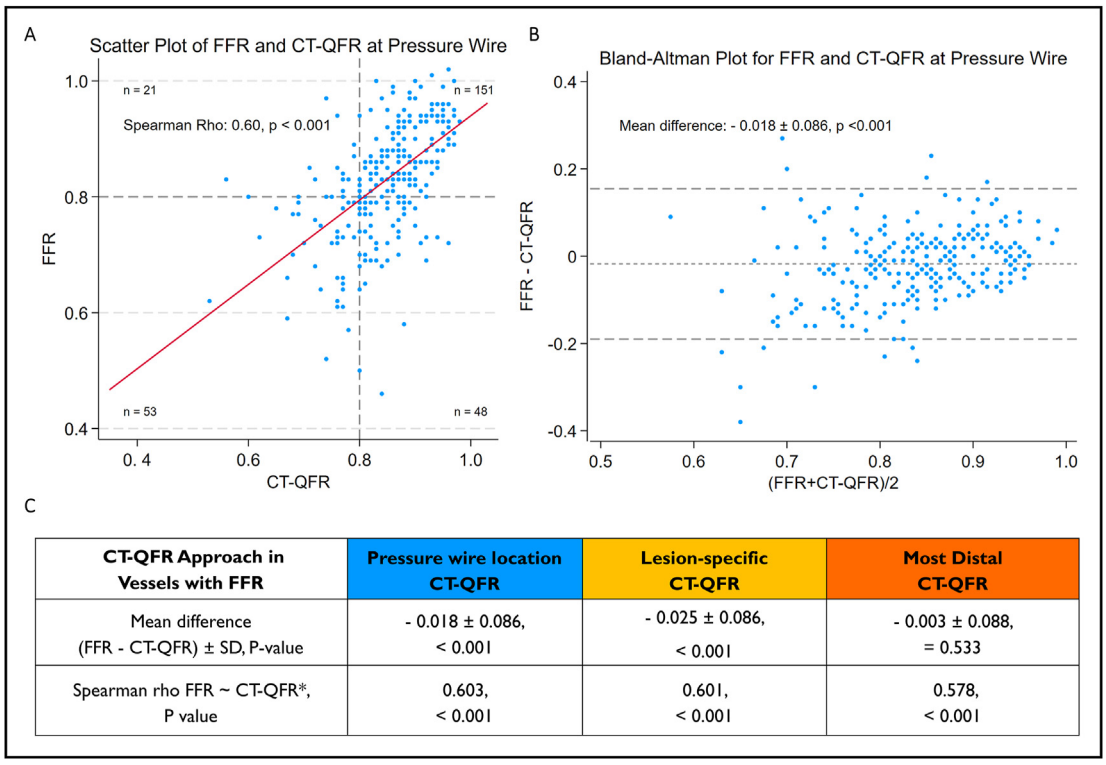

CT-QFR Approach in Vessels with FFR	Pressure wire location CT-QFR	Lesion-specific CT-QFR	Most Distal CT-QFR
Mean difference (FFR - CT-QFR) ± SD, P-value	- 0.018 ± 0.086, < 0.001	- 0.025 ± 0.086, < 0.001	- 0.003 ± 0.088, = 0.533
Spearman rho FFR ~ CT-QFR*, P value	0.603, < 0.001	0.601, < 0.001	0.578, < 0.001

Fig. 3. Scatter and Bland-Altman plots - CT-QFR and FFR at pressure wire location. A) Scatterplot over pressure wire location CT-QFR values and invasive FFR values, demonstrating a moderate correlation to invasive FFR. B) Bland-Altman Plot demonstrating that Pressure wire CT-QFR slightly overestimated FFR with narrow limits of agreements, which contained >95 % of measurements. C) Table showing Mean difference and Spearman correlations between CT-QFR and FFR.

4.1. Current CT-QFR iteration compared to previous CT-QFR studies

In this study, the use of CT-QFR was investigated as a non-invasive second-line alternative for discrimination of hemodynamically obstructive CAD in patients with suspected stenosis on CCTA. We found sensitivities of 77–80 % and specificities of 73–80 % which is somewhat different from previous retrospective studies reporting higher sensitivities and comparable specificities.[9,15] Overall, several explanations are possible including that previous studies 1) exclusively utilized MD-QFR values that in alignment with our findings overestimates CT-QFR compared with invasive FFR[9]; 2) applied experienced core-lab CT-QFR reads with core-lab reads being more precise[15,24]; and 3) only included CT-QFR from vessels with invasive FFR measurements and disregarded the CT-QFR from other vessels. The latter is not applicable in a real-world setting where all major coronary vessels should be evaluated prior to invasive referral using the second-line non-invasive approach of choice, which is the reason that the present study included CT-QFR assessment for all arteries >1.5 mm. Further, as incorrect lumen contouring affects CT-QFR, underestimation of diameter stenosis severity or overestimation of minimal lumen diameter could partly explain overestimation of invasive FFR in the present study (Table S2). Other potentially contributing factors explaining our observed impaired sensitivity are patient selection as our patients were selected due to a suspected stenosis on CCTA, and previous studies applied different definitions of obstructive CAD. Similar to our findings, Li et al. reported comparable diagnostic accuracy in vessels with localized extensively calcified lesions.[9,15]

4.2. CT-QFR compared to other functional CT-assessments

Compared to previous studies on other computational fluid dynamic models (i.e., CT derived Fractional Flow Reserve (FFRct)), we found similar overall diagnostic accuracy of CT-QFR; 77–80 % vs. 78–81 % of FFRct in the NXT trial and post hoc analysis of the PACIFIC trial.[25,26] However, our reported AUCs of MD-QFR and LS-QFR were both lower (0.83 and 0.85) compared to FFRct (0.90–0.92) as FFRct typically underestimates invasive FFR in contrast to CT-QFR which typically overestimates invasive FFR.[9,14,15] In general, the differences in diagnostic performance between CT-QFR and FFRct can be attributed to several factors. Firstly, CT-QFR and FFRct apply different computational approaches, with FFRct including a highly comprehensive fluid dynamics model that simulates blood flow in the coronary arteries while also incorporating myocardial mass in the estimation of invasive FFR.[27] In contrast, CT-QFR patient-specific resting coronary flow was estimated using the reference arterial volume according to the allometric scaling law and converted to virtual hyperemic flow.[21] Secondly, disease severity, disease prevalence and reference standards of choice vary between previous FFRct studies. Thirdly, previous FFRct studies had rather strict image quality criteria and excluded 13–25 % of patients[25,26] whereas only 5 % of patients were excluded for CT-QFR analysis in the present study. Fourthly, spectrum bias is a possibility as previous FFRct studies included symptomatic patients primarily referred for ICA while our results are based on low-intermediate risk patients with initial clinical indication for CCTA.[28] Adding to this point, a recent real-life study showed a marked decrease in predictive values of FFRct performance in patients initially referred for CCTA.[29] Overall, previous FFRct studies only applied values extracted at the position of the pressure wire, and while this method has academic merit for validation, it does not provide a patient-centred non-invasive approach of how to use computational FFR. In this study of CT-QFR, we showed that using LS-QFR may have small incremental advantages over using MD-QFR for safely reducing the number of unnecessary ICAs that are not followed by revascularization, while FFRct performance varies substantially according to measurement site.[28]

4.3. CT-QFR feasibility and clinical perspectives

CT-QFR is a fast and feasible second-line imaging technique that takes less than 10 min to perform.[15] Compared to e.g., FFRct, CT-QFR can be performed on-site in the same session as performing a clinically indicated CCTA examination without the need for image transfer.[29]

While core-lab interpreted MD-QFR has shown promise as a non-invasive tool for assessing hemodynamically obstructive CAD,[9,14,15] our findings demonstrate that both MD-QFR and LS-QFR calculated on-site has a sensitivity >75 % to identify hemodynamically obstructive lesions by ICA in patients with CCTA stenosis of ≥50 %, with a high negative predictive value above 85 % in case of normal CT-QFR (Fig. 2). Authors report even lower sensitivities against hemodynamically obstructive CAD by different myocardial perfusion imaging techniques, especially in invasive FFR grey-zone patients.[14,18,26] Importantly, both MD-QFR and LS-QFR identified the vast majority of patients (>95 %) with multi-vessel obstructive CAD.

Although CCTA generally overestimates stenosis severity,[5] the current semi-automatic lumen detection by the CT-QFR software may underestimate stenosis severity, concomitantly leading to higher CT-QFR values (Supplementary Figure 3). This suboptimal lumen boundary detection may be reduced by increased reader experience, on-site collaboration with core lab expert readers and improvements in the artificial intelligence guided lumen contouring algorithm, this should be evaluated in future prospective CT-QFR studies. Instead of CCTA anatomical diameter stenosis alone to guide invasive referral, CT-QFR could reduce more than half the number of invasive referrals. Such scenario could hypothetically almost double revascularization rates to 70 % by LS-QFR compared to 37 % by CCTA alone while the majority of patients (>84 %) with a normal CT-QFR could safely be deferred from unnecessary ICAs as no hemodynamically obstructive lesions were identified (Fig. 2, Graphical abstract, Figure S1). This should be tested in a prospective trial evaluating CT-QFR compared to invasive FFR, ideally with measurements of both in all major vessels.

4.4. Limitations

Our study has some limitations. First, not all vessels had invasive FFR, and using more severe 70 % DS by 3D-QCA may have decreased the specificity of CT-QFR. However, the 70 % DS threshold is in accordance with guidelines on revascularization stating that such lesions per definition cause myocardial ischemia.[30] Secondly, to reflect the clinical approach of adapting CT-QFR to an on-site read, we utilized a single trained analyst without repeated measurements and with less experience than external core lab interpreters; however, repeated measurements have previously demonstrated small intra- and inter-observer variability and good intra-class correlations.[15] Thirdly, although the Dan-NICAD trial had pre-specified investigations of both CT-derived FFR and invasive QFR against obstructive CAD on ICA, the present CT-QFR analysis was performed post-hoc. Finally, we included only patients with suspected obstructive CAD on CCTA and while this approach is in accordance with guidelines,[3] it may have resulted in a high prevalence of borderline disease in our population compared to patients primarily referred for ICA.

5. Conclusions

To conclude, in an all-comer population, on-site CT-QFR showed good feasibility and good diagnostic accuracy for detecting hemodynamically obstructive CAD. Overall, CT-QFR tended to be overestimated compared to invasive FFR. Despite a modest reclassification potential, using lesion-specific CT-QFR had improved diagnostic accuracy over the conventional most distal CT-QFR approach. Normal CT-QFR could exclude hemodynamically obstructive CAD in the majority of patients.

Data availability statement

The data forming the basis of this article can be shared upon reasonable request, at the discretion of the study sponsor and primary investigator (MB) and within the bounds of the Danish Data Protection Agency.

Funding

Jonathan Nørtoft Dahl acknowledges unrestricted research grant from the Research Foundation at Gødstrup Hospital. Laust Dupont Rasmussen acknowledges support from Danish Cardiovascular Academy (grant number PD5Y-2023001-DCA), which is funded by the Novo Nordisk Foundation (grant number NNF20SA0067242) and The Danish Heart Foundation. William Wijns acknowledges support to a Research Professorship grant from Science Foundation Ireland (15/RP/2765).

The remaining authors have nothing to disclose.

Declaration of competing interest

Morten Bøttcher reports advisory board participation for NOVO Nordisk, Astra-Zeneca, Pfizer, Boeringer Ingelheim, Bayer, Sanofi, Novartis, Amgen, CLS-Behring, Acarix and MEDtrace. William Wijns reports senior advisor Rede Optimus Research and Corrib Core Laboratory, co-founder Argonauts Partners, an innovation facilitator. Shengxian Tu reports consultancy and research grants from Pulse Medical.

Acknowledgements

We would like to express our sincere appreciation to the study nurses and participating Dan-NICAD patients for their invaluable contribution. We also extend our gratitude to Jesper Thygesen, chief engineer at the CT unit Aarhus University Hospital for his assistance in the data handling and CCTA retrieval process.

Appendix A. Supplementary data

Supplementary data to this article can be found online at https://doi.org/10.1016/j.jcct.2024.01.004.

References

1. Moss AJ, Williams MC, Newby DE, Nicol ED. The updated NICE guidelines: cardiac CT as the first-line test for coronary artery disease. *Curr Cardiovasc Imaging Rep*. 2017;10:15.
2. Knuuti J, Wijns W, Saraste A, et al. 2019 ESC Guidelines for the diagnosis and management of chronic coronary syndromes. *Eur Heart J*. 2020;41:407–477.
3. Writing Committee M, Gulati M, Levy PD, et al. 2021 AHA/ACC/ASE/CHEST/SAEM/SCCT/SCMR guideline for the evaluation and diagnosis of chest pain: a report of the American College of Cardiology/American heart association joint committee on clinical practice guidelines. *J Am Coll Cardiol*. 2021;78:e187–e285.
4. Meijboom WB, Van Mieghem CA, van Pelt N, et al. Comprehensive assessment of coronary artery stenoses: computed tomography coronary angiography versus conventional coronary angiography and correlation with fractional flow reserve in patients with stable angina. *J Am Coll Cardiol*. 2008;52:636–643.
5. Nissen L, Winther S, Schmidt M, et al. Implementation of coronary computed tomography angiography as nationally recommended first-line test in patients with suspected chronic coronary syndrome: impact on the use of invasive coronary angiography and revascularization. *Eur Heart J Cardiovasc Imaging*. 2020;21:1353–1362.
6. Shaw LJ, Blankstein R, Bax JJ, et al. Society of cardiovascular computed tomography/North American society of cardiovascular imaging - expert consensus document on coronary CT imaging of atherosclerotic plaque. *J Cardiovasc Comput Tomogr*. 2021;15:93–109.
7. Tu S, Westra J, Yang J, et al. Diagnostic accuracy of fast computational approaches to derive fractional flow reserve from diagnostic coronary angiography: the international multicenter FAVOR pilot study. *JACC Cardiovasc Interv*. 2016;9:2024–2035.
8. Yu W, Tanigaki T, Ding D, et al. Accuracy of intravascular ultrasound-based fractional flow reserve in identifying hemodynamic significance of coronary stenosis. *Circ Cardiovasc Interv*. 2021;14:e009840.

9. Li Z, Zhang J, Xu L, et al. Diagnostic accuracy of a fast computational approach to derive fractional flow reserve from coronary CT angiography. *JACC Cardiovasc Imaging*. 2020;13:172–175.
10. Yu W, Huang J, Jia D, et al. Diagnostic accuracy of intracoronary optical coherence tomography-derived fractional flow reserve for assessment of coronary stenosis severity. *EuroIntervention*. 2019;15:189–197.
11. Cortes C, Carrasco-Moraleja M, Aparisi A, et al. Quantitative flow ratio-Meta-analysis and systematic review. *Cathet Cardiovasc Interv*. 2021;97:807–814.
12. Biscaglia S, Tebaldi M, Brugaletta S, et al. Prognostic value of QFR measured immediately after successful stent implantation: the international multicenter prospective HAWKEYE study. *JACC Cardiovasc Interv*. 2019;12:2079–2088.
13. Xu B, Tu S, Song L, et al. Angiographic quantitative flow ratio-guided coronary intervention (FAVOR III China): a multicentre, randomised, sham-controlled trial. *Lancet*. 2021;398:2149–2159.
14. Westra J, Li Z, Rasmussen LD, et al. One-step anatomic and function testing by cardiac CT versus second-line functional testing in symptomatic patients with coronary artery stenosis: head-to-head comparison of CT-derived fractional flow reserve and myocardial perfusion imaging. *EuroIntervention*. 2021;17:576–583.
15. Li Z, Li G, Chen L, et al. Comparison of coronary CT angiography-based and invasive coronary angiography-based quantitative flow ratio for functional assessment of coronary stenosis: a multicenter retrospective analysis. *J Cardiovasc Comput Tomogr*. 2022;16:509–516.
16. Cami E, Tagami T, Raff G, et al. Assessment of lesion-specific ischemia using fractional flow reserve (FFR) profiles derived from coronary computed tomography angiography (FFRCT) and invasive pressure measurements (FFRINV): importance of the site of measurement and implications for patient referral for invasive coronary angiography and percutaneous coronary intervention. *J Cardiovasc Comput Tomogr*. 2018;12:480–492.
17. Rasmussen LD, Winther S, Westra J, et al. Danish study of Non-Invasive testing in Coronary Artery Disease 2 (Dan-NICAD 2): study design for a controlled study of diagnostic accuracy. *Am Heart J*. 2019;215:114–128.
18. Rasmussen LD, Winther S, Eftekhari A, et al. *Second-Line Myocardial Perfusion Imaging to Detect Obstructive Stenosis: Head-To-Head Comparison of CMR and PET*. JACC Cardiovasc Imaging; 2023.
19. Bischoff B, Hein F, Meyer T, et al. Impact of a reduced tube voltage on CT angiography and radiation dose: results of the PROTECTION I study. *JACC Cardiovasc Imaging*. 2009;2:940–946.
20. Raff GL, Abidov A, Achenbach S, et al. SCCT guidelines for the interpretation and reporting of coronary computed tomographic angiography. *J Cardiovasc Comput Tomogr*. 2009;3:122–136.
21. Tu S, Ding D, Chang Y, Li C, Wijns W, Xu B. Diagnostic accuracy of quantitative flow ratio for assessment of coronary stenosis significance from a single angiographic view: a novel method based on bifurcation fractal law. *Cathet Cardiovasc Interv*. 2021; 97(Suppl 2):1040–1047.
22. Norgaard BL, Fairbairn TA, Safian RD, et al. Coronary CT angiography-derived fractional flow reserve testing in patients with stable coronary artery disease: recommendations on interpretation and reporting. *Radiol Cardiothorac Imaging*. 2019; 1:e190050.
23. Kosinski AS. A weighted generalized score statistic for comparison of predictive values of diagnostic tests. *Stat Med*. 2013;32:964–977.
24. Lu MT, Meyersohn NM, Mayrhofer T, et al. Central core laboratory versus site interpretation of coronary CT angiography: agreement and association with cardiovascular events in the PROMISE trial. *Radiology*. 2018;287:87–95.
25. Norgaard BL, Leipsic J, Gaur S, et al. Diagnostic performance of noninvasive fractional flow reserve derived from coronary computed tomography angiography in suspected coronary artery disease: the NXT trial (Analysis of Coronary Blood Flow Using CT Angiography: next Steps). *J Am Coll Cardiol*. 2014;63:1145–1155.
26. Driessen RS, Danad I, Stuijfzand WJ, et al. Comparison of coronary computed tomography angiography, fractional flow reserve, and perfusion imaging for ischemia diagnosis. *J Am Coll Cardiol*. 2019;73:161–173.
27. Min JK, Taylor CA, Achenbach S, et al. Noninvasive fractional flow reserve derived from coronary CT angiography: clinical data and scientific principles. *JACC Cardiovasc Imaging*. 2015;8:1209–1222.
28. Cami E, Tagami T, Raff G, et al. Importance of measurement site on assessment of lesion-specific ischemia and diagnostic performance by coronary computed tomography Angiography-Derived Fractional Flow Reserve. *J Cardiovasc Comput Tomogr*. 2021;15:114–120.
29. Mittal TK, Hothi SS, Venugopal V, et al. *The Use and Efficacy of FFR-CT: Real-World Multicenter Audit of Clinical Data with Cost Analysis*. JACC Cardiovasc Imaging; 2023.
30. Lawton JS, Tamis-Holland JE, Bangalore S, et al. 2021 ACC/AHA/SCAI guideline for coronary artery revascularization: executive summary: a report of the American College of Cardiology/American heart association joint committee on clinical practice guidelines. *Circulation*. 2022;145:e4–e17.